Available online at www.sciencedirect.com
SCIENCE DIRECT®
ELSEVIER
Nuclear Instruments and Methods in Physics Research A 527 (2004) 201–205
NUCLEAR INSTRUMENTS & METHODS IN PHYSICS RESEARCH Section A
www.elsevier.com/locate/nima

A full Monte Carlo simulation of the YAP-PEM prototype for breast tumor detection

A. Motta[a,*], S. Righi[a], A. Del Guerra[a], N. Belcari[a], A. Vaiano[a], G. Di Domenico[b], G. Zavattini[b], R. Campanini[c], N. Lanconelli[c], A. Riccardi[c]

[a] *University of Pisa and INFN of Pisa, Pisa, Italy*
[b] *University of Ferrara and INFN of Ferrara, Ferrara, Italy*
[c] *University of Bologna and INFN of Bologna, Bologna, Italy*

Abstract

A prototype for Positron Emission Mammography, the YAP-PEM, is under development within a collaboration of the Italian Universities of Pisa, Ferrara, and Bologna. The aim is to detect breast lesions, with dimensions of 5 mm in diameter, and with a specific activity ratio of 10:1 between the cancer and breast tissue. The YAP-PEM is composed of two stationary detection heads of $6 \times 6\,cm^2$, composed of a matrix of 30×30 YAP:Ce finger crystals of $2 \times 2 \times 30\,mm^3$ each. The EGSnrc Monte Carlo code has been used to simulate several characteristics of the prototype. A fast EM algorithm has been adapted to reconstruct all of the collected lines of flight, also at large incidence angles, by achieving 3D positioning capability of the lesion in the FOV. The role of the breast compression has been studied. The performed study shows that a 5 mm diameter tumor of $37\,kBq/cm^3$ ($1\,\mu Ci/cm^3$), embedded in active breast tissue with 10:1 tumor/background specific activity ratio, is detected in 10 min with a Signal-to-Noise Ratio of 8.7 ± 1.0. Two hot lesions in the active breast phantom are clearly visible in the reconstructed image.

PACS: 87.53.Wz; 87.57.Ce; 87.57.Gg; 87.58.Fg; 87.59.Ek

Keywords: PEM; Mammography

1. Introduction

A dedicated camera for Positron Emission Mammography (PEM) offers high sensitivity and high spatial resolution in the detection of small non-palpable breast cancers, with dimensions of less than 5 mm.

Compared to whole body PET cameras, dedicated devices allow a better, easier and flexible positioning around the breast, a simple application of compression, and the integration with RX cameras. The positioning in the vicinity of the tumor implies, firstly, larger solid angle coverage, increased sensitivity, and the exclusion of the thorax from the camera Field of View (FOV), resulting in a background reduction. The coupling of a high density crystal matrix with Position Sensitive Photomultiplier Tubes (PSPMTs) gives high detection efficiency and high spatial

*Corresponding author. Tel.: +39-050-2214334; fax: +39-050-2214333.
E-mail address: motta@df.unipi.it (A. Motta).

0168-9002/$ - see front matter © 2004 Elsevier B.V. All rights reserved.
doi:10.1016/j.nima.2004.03.120

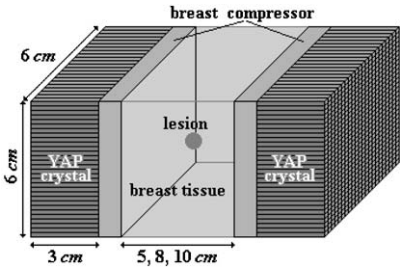

Fig. 1. YAP-PEM prototype design.

resolution (<3 mm FWHM). The reduced number of camera components also allows a notable reduction of cost.

2. The YAP-PEM prototype

The adopted technology derives from our previous experience with a small animal imaging scanner [1,2]. The YAP-PEM is based on Yttrium Aluminum Perovskite (YAP:Ce) crystal matrices coupled to PSPMTs. Two opposite stationary detection heads of $6 \times 6\,cm^2$ are composed by a matrix of 30×30 YAP:Ce finger crystals of $2 \times 2 \times 30\,mm^3$ each (Fig. 1).

The breast compression increases the lesion visibility [3], especially for the most dangerous cancers lying near the thorax; therefore each head is equipped with a compressor of 1 cm thick Perspex. A 50 μm tungsten sheet will be placed between the crystal matrix and the compressor to shield the background of low-energy photons. The distance between the two heads ranges from 5 up to 10 cm, depending on the breast compression, and determines the axial dimension of the FOV.

3. Simulation and reconstruction software

The EGSnrc Monte Carlo code has been used to simulate spherical lesions positioned inside a uniform slab of breast tissue, whose chemical and physical characterization is given by ICRU-44. In our simulations, a compression status of mild, moderate, and strong corresponds to compressor distances of 10, 8 and 5 cm, respectively. Scattering events from the thorax (outside the FOV) are not simulated. We have assumed a specific activity of $37\,kBq/cm^3$ ($1.0\,\mu Ci/cm^3$) for tumors, and of $3.7\,kBq/cm^3$ ($0.1\,\mu Ci/cm^3$) for the biological breast tissue, i.e. a 10:1 tumor/background (T/B) ratio. An acquisition time of 10 min was used in all cases. The positron source is the ^{18}F radioisotope. No simulation of the PSPMT readout is performed.

Particles have been transported with several energy cut-offs: 50 keV for photons and electrons in the FOV; 10 keV for photons in the YAP crystal. Electron transport within the detector has not been performed. Energy depositions (E) have been folded with the appropriate resolution, scaled as $(E)^{-1/2}$ from the value of 25% at 511 keV, previously measured with the YAP-PET tomograph [1]. For multiple energy depositions, the photon interaction coordinates are determined by energy weighting.

The developed simulation code has been validated by comparison with experimental results.

A fast EM algorithm has been adapted from the reconstruction program developed for the small animal tomograph YAP-PET [4,5]. The imaging needs 30 s/iteration on a PC-Pentium III 800 MHz processor; due to the quasi-planar nature of the data, the solution is obtained at the first iteration. The EM algorithm allows one to use all of the *lines of response* (LORs) in the FOV: the greatest inclination of an accepted LOR depends on the compressor distance, and ranges from 30° to 50°, for mild and strong compression, respectively. It would not be possible to use all of the LORs with Filtered Backprojection reconstruction.

4. Monte Carlo validation

We had the opportunity to validate the Monte Carlo code, by comparing with the experimentally acquired data from the small animal tomograph YAP-PET. The simulation of a cylindrical source of equal height and diameter of 3 mm (Fig. 2), of 10 nCi, with a 10:1 tumor/background (T/B) ratio, gives an SNR value of 9.4 ± 1.4; the experimental acquisition of the corresponding solid phantom in the same geometry gives $SNR = 9.0 \pm 1.5$.

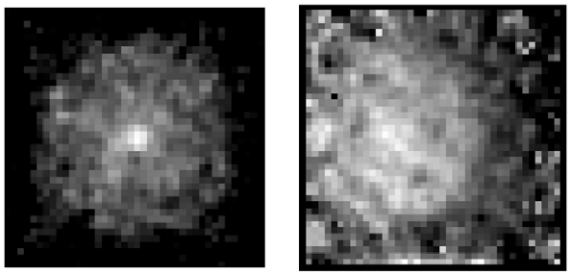

Fig. 2. A Monte Carlo simulation (left) of a phantom experimentally acquired with the YAP-PET tomograph (right).

5. Results of Monte Carlo simulations

The first study analyzes the visibility of the tumor with respect to its size, by varying the lesion volume from 1.0 cm^3 (12.4 mm diameter) down to 0.065 cm^3 (5.0 mm), with strong compression (Fig. 3, top). The SNR values (Fig. 3, bottom) are measured from the reconstructed images (1 mm slices), by using the definition $SNR = (T-B)/\sigma_B$, where T and B are the average signal from the tumor and from the normal tissue, respectively, and σ_B is the standard deviation of B.

The SNR values depend on the acceptance energy window (Fig. 4, for a 5 mm diameter (0.065 cm^3) tumor, with strong compression).

The effect of compression has been simulated by varying the detection head distances: 5, 8 and 10 cm for strong, moderate and mild compression, respectively. We consider the breast as an incompressible fluid. Fig. 5 shows the results for the 5.0 mm diameter tumor.

The dependence of the detectability of a tumor on its position within the FOV is shown in Fig. 6. The 0.5 cm^3 tumor (9.8 mm diameter) has been positioned at the center of the strong compression FOV and then translated by 1 cm steps on the central plane along the axis parallel to both detector faces. A similar result (not shown here) has been obtained for displacement along the orthogonal axis. The energy window used is 50–650 keV.

A study has been performed by simulating two lesions of 5 mm diameter in the active breast tissue (Fig. 7), with a 10:1 T/B ratio, with strong

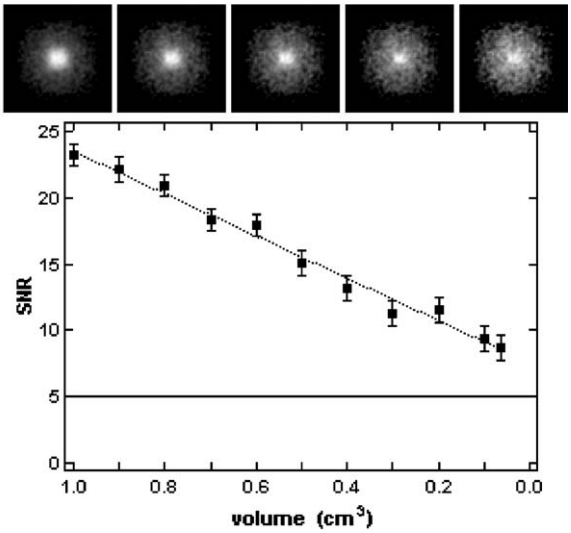

Fig. 3. (Top) Images of lesion with decreasing volume (diameter): from the left, 1.0 cm^3 (12.4 mm), 0.5 cm^3 (9.8 mm), 0.3 cm^3 (8.4 mm), 0.1 cm^3 (5.8 mm), and 0.065 cm^3 (5.0 mm). The tumor lies at the FOV center in active breast tissue, with a 10:1 T/B ratio. The compression is strong. Reconstructed data are within a 50–650 keV energy window. All the images are in 256 gray-scale, from a reference background value to its own maximum. (Bottom) SNR values obtained from reconstructed images of simulated tumors, whose sizes vary from a 1.0 cm^3 volume down to 0.065 cm^3 (5.0 mm). The SNR equal to 5 line, i.e. the conventional limit of visibility in analog radiology, is also reported.

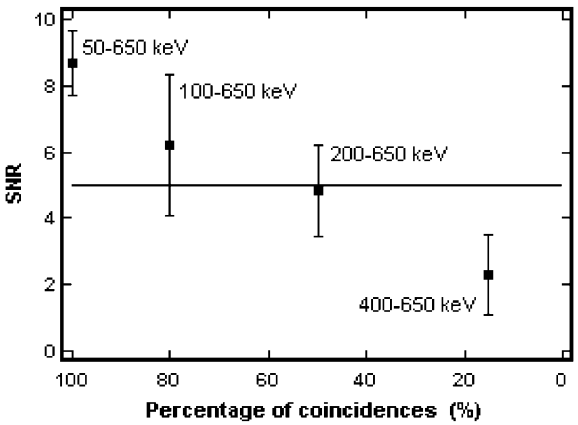

Fig. 4. Effect of the width of the energy window of LOR acceptance, applied to both detectors, for a 5.0 mm diameter tumor, in strong compression.

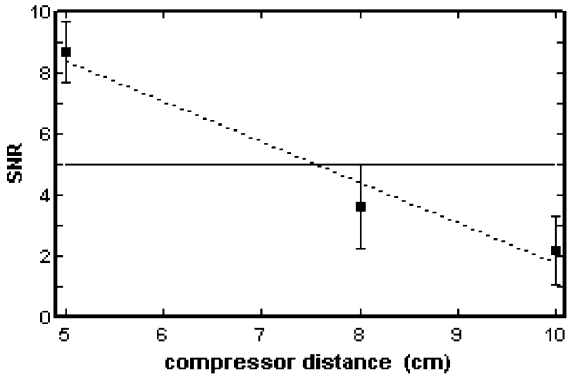

Fig. 5. SNR values for different breast compressions. Three compressor distances of 5, 8, and 10 cm are considered, for strong, moderate and mild compression. The tumor has a diameter of 5 mm. A 50–650 keV energy window has been applied to both detectors.

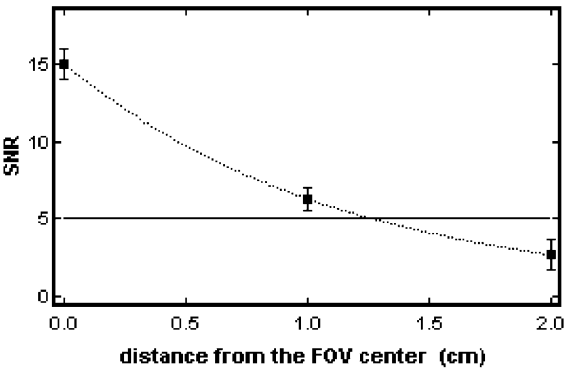

Fig. 6. Tumor detectability as a function of distance from the center of the FOV, along the axis parallel to the detector plane (a). The tumor has a volume of 0.5 cm^3 (9.8 mm diameter). An energy window of 50–650 keV is applied, for a strong compression condition.

compression. An acceptance energy window of 50–650 keV has been applied.

6. Discussion and conclusion

The developed Monte Carlo simulator has been fully validated by comparing with the experimental data obtained with the YAP-PET (Fig. 2).

The Monte Carlo simulation indicates that the YAP-PEM prototype will be able to detect, with an SNR of 8.7 ± 1.0, a 5 mm diameter (0.065 cm^3) tumor of 37 kBq/cm^3, in active breast tissue with a 10:1 T/B ratio, with a 10 min acquisition, for a compressor distance of 5 cm (Fig. 3).

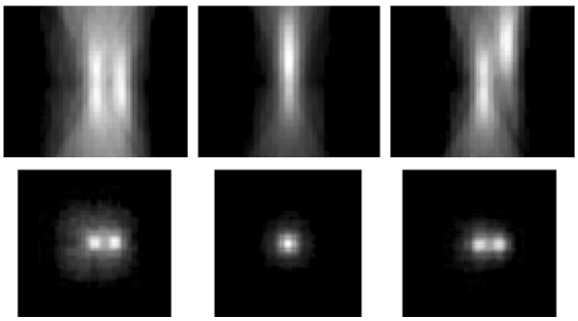

Fig. 7. Two hot sources of 5 mm diameter are embedded in active breast tissue, with a 10:1 T/B ratio. The images are 3D, scaled in 256 gray-scale, from a reference value of background to its own maximum: (top row) central slice parallel to the camera axis; (bottom row) central slice orthogonal to the axis. (Left column) The lesions lie in the same plane, parallel to the two detector surfaces, at the FOV center. (Middle column) The lesions lie onto the camera axis. (Right column) The two preceding displacements are combined.

The simulation of spherical tumors with different diameters suggests that the measured SNR values depend linearly on the tumor volume size (Fig. 3).

The SNR values are strongly dependent on the acquired statistics. The reduction of the width of the energy window, applied to both of the detectors, reduces the measured SNR (Fig. 4): the lowest energy threshold enhances the detectability of the tumor. We expect that this could change when the scatter from thorax is considered.

This study confirms the important role of breast compression (Fig. 5), especially to detect the smallest tumors (<0.1 cm^3).

The background from breast tissue activity compromises the detectability of tumors lying far from the FOV center. A 0.5 cm^3 (9.8 mm) tumor is always detectable within a 1.0 cm distance from the FOV center; but its measured SNR decreases under the value of 5 at a distance of just 2 cm from the center (Fig. 6). This would indicate that with a T/B ratio of 10:1, the 6×6 cm^2 active area assures high detectability in the central 4×4 cm of the FOV; outside this area the tumor detectability has an SNR of less than 5.

The prototype will be able to clearly discriminate two hot sources of 5.0 mm diameter (Fig. 7) if they do not lie on the same axis; otherwise, the camera sees only a source in the median plane.

References

[1] A. Del Guerra, C. Damiani, G. Di Domenico, M. Giganti, R. Marchesini, A. Motta, A. Piffanelli, N. Sabba, L. Sartori, G. Zavattini, IEEE Trans. Nucl. Sci. NS-47 (2000) 1537.

[2] G. Di Domenico, A. Motta, G. Zavattini, A. Del Guerra, C. Damiani, V. Bettinardi, M.C. Gilardi, Nucl. Instr. and Meth. A 477 (2002) 505.

[3] R. Pani, A. Soluri, I.N. Weinberg, G. De Vincentis, R. Scafé, M.N. Cinti, L. Indovina, F. Scopinaro, V. David, F. Garibaldi, A. Del Guerra, I. Khalkhali, Conference Records of the IEEE Nuclear Science Symposium and Medical Imaging Conference 2000, Lyon, France, 15–20 October 2000, ISBN-0-7803-6506-2 (CD-ROM), (2001) 2696.

[4] A. Motta, (Ph.D. Thesis Abstract) Med. Phys. 28(6) (2001) 1141.

[5] A. Motta, C. Damiani, A. Del Guerra, G. Di Domenico, G. Zavattini, Comput. Med. Imag. Graph. 26 (2002) 293.